



Optimization of perfluorosulfonic acid ionomer loadings in catalyst layers of proton exchange membrane fuel cells

Shichun Mu*, Mingxing Tian

State Key Laboratory of Advanced Technology for Materials Synthesis and Processing, Wuhan University of Technology, Wuhan 430070, China

ARTICLE INFO

Article history:

Received 14 July 2011

Received in revised form

22 November 2011

Accepted 24 November 2011

Available online 6 December 2011

Keywords:

Proton exchange membrane fuel cell

Catalyst layer

Perfluorosulfonic acid ionomer

Loadings

ABSTRACT

The effect of perfluorosulfonic acid ionomer loadings on electrochemical surface area, gas transfer resistance and output voltage performance was systematically studied by both electrochemical and fuel cell experiments. Differently from the previous reports, a high Pt loading catalyst (60 wt.% Pt/C) was used to evaluate the effect in this work. The optimum loading of perfluorosulfonic acid ionomers in catalyst layers was determined. It was found that the ionomer anode content slightly influenced single cell performance and the optimum ionomer anode loading was 30 wt.%. Based on reasonable gas transfer resistance and fuel cell performance, the optimum ionomer cathode loading was 25–30 wt.%. Significantly, the optimum loading of the ionomer showed a nondependence relationship with Pt loadings in catalyst layers.

© 2011 Elsevier Ltd. All rights reserved.

1. Introduction

Ionomers have been used in proton exchange membrane fuel cells (PEMFCs) to enhance the proton conductivity of catalyst layers and membranes. The most commonly used ionomer in PEMFCs is the perfluorosulfonic acid, such as Nafion®. The Nafion percentage (NFP) in catalyst layers is one of most important factors to determine Pt catalyst utilization rate. The proton conductivity of catalyst layers would decrease at too low NFP, leading to a low catalyst utilization rate and a high impedance of the membrane electrode assembly (MEA). On the other hand, the gas transport and electricity conductivity would be low at too high NFP, corresponding to a low catalyst utilization rate [1–3]. Thus, the NFP value should be controlled in a reasonable range. Recently, 20–40 wt.% Pt/C has been widely used in catalyst layers in the determination of the optimum NFP values [4–9]. However, the current tendency is towards higher Pt loading catalysts (60 wt.% Pt/C or over) used in PEMFCs due to the higher catalytic efficiency [10,11]. Therefore, in the process of increasing the Pt loading of catalysts, the optimum NFP has to be reconsidered. Moreover, most studies have focused on evaluation of NFP in catalyst layers under the same Pt loading because of requirements of consistent results. Thus far, the effect of NFP at both the anode and the cathode sides on single cell performances has not been systematically studied. In addition, there have long been questions

regarding whether or not the presence of optimum NFP at different Pt loading in catalyst layers. We have noticed that there presents no direct relationship between the Pt loading and optimum NFP in most cases through comparative studies of Refs. [1,4,7,8]. However, the previous studies did not clearly state this nondependence relationship, in contrast, a few researchers [5,6] have taken the opposite point of view that the optimum NFP should depend on the Pt loading. Therefore, in this work, the most favorable NFP and relationship between the Pt loading and optimum NFP in higher Pt loading catalyst (60 wt.% Pt/C) are investigated through the combination studies of electrochemical and single cell experiments.

2. Experimental

The membrane electrode assembly (MEA) was prepared by the catalyst-coated membrane (CCM) method [12,13]. 60 wt.% Pt/C electrocatalyst (Hispec™ 9100) was purchased from Johnson Matthey Corp. Ionomer solution (5 wt.% Nafion® solution), and Nafion® 211 membranes with thickness of 25 μm were obtained from Du Pont. Gas diffusion layers with water management layers were provided by WUT Energy Co. All solutions were prepared with deionized water of resistivity not less than 18.2 MΩ cm⁻².

Multiple CCMs were prepared according to the catalyst loadings in catalyst layers. Samples with the different NFP of 10, 20, 25, 30, 40 and 50 wt.% on test electrode sides at the same Pt loading of 0.35 mg cm⁻² were prepared. Another samples with the NFP of 20, 30 and 40 wt.% on test electrode sides at Pt loadings of 0.15 and 0.5 mg cm⁻², respectively, were also prepared. As

* Corresponding author. Tel.: +86 27 87651837x8611; fax: +86 27 87879468.

E-mail addresses: mshc@whut.edu.cn, mushichun@gmail.com (S. Mu).

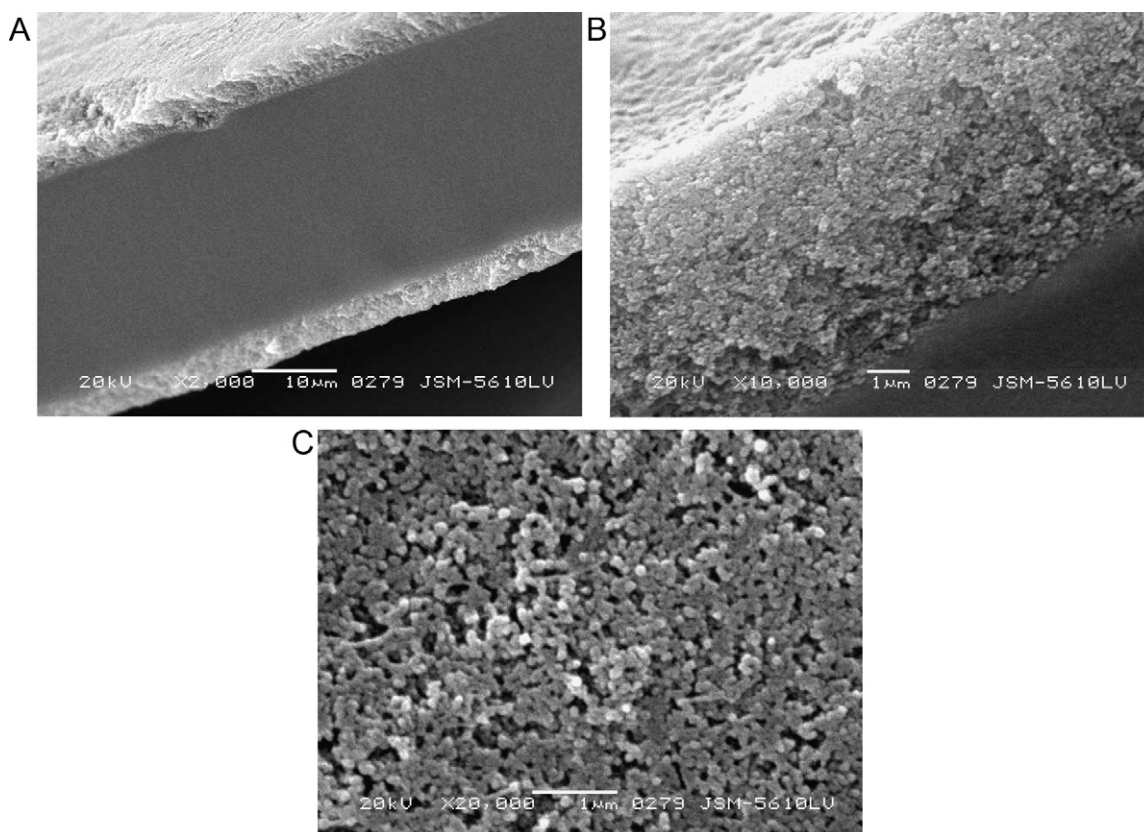


Fig. 1. SEM images of the cross-section (A), magnified cross-section (B), and surface (C) of catalyst layers for CCMs.

a benchmark, the NFP of 25 wt.% on the reference (or counter) electrode side with 0.4 mg cm^{-2} Pt loading was employed. The prepared CCMs were assessed by single cells with active area $5 \text{ cm}^{-1} \times 5 \text{ cm}^{-1}$.

Single cell testing has been performed by G50 Fuel Cell Test Station (GreenLight) with H_2 as fuel feed gas and air/ O_2 as oxidant and without back pressure. H_2 stoic was 1.5 at anode and air (or O_2) stoic was 2.0 at cathode. The humidity was 100% RH at both electrode sides and controlled by dew-point temperature at 60°C . Prior to the measurement, cells were activated by polarization at a constant current till a stable performance was obtained.

Cyclic voltammetric measurements of single cells were carried out using a three electrode configuration by an Autolab (PGSTA30, The Netherlands) potentiostat. The test electrode was employed as the working electrode at a fixed N_2 gas flow rate of 10 sccm (100% RH) and the other electrode was as the counter electrode at a fixed H_2 gas flow rate of 20 sccm (100% RH). The counter electrode was also served as a reference electrode because the overpotential at the counter electrode for the hydrogen oxidation or evolution reaction was negligible [14]. The measurement was carried out at the scan rate of 50 mV/s in a potential window of $0.05\text{--}1.25 \text{ V}$ vs. RHE at room temperature after 2-h activation. The electrochemically active surface area (ECSA) was calculated using the following equation [15,16]

$$\text{ECSA} = \frac{Q_H}{m \times q_H} \quad (2.2)$$

where Q_H is charge for Hupd adsorption, m is the loading of metal, and q_H ($210 \mu\text{C cm}^{-2}$) is the charge required for monolayer adsorption of hydrogen on Pt surfaces.

3. Results and discussion

3.1. Morphology of catalyst layers

Fig. 1A illustrates the SEM image of typical cross-section of CCM. The middle part is Nafion® 211 membrane with thickness of $25 \mu\text{m}$. The bilateral catalyst layers are composed of the Pt/C catalyst and perfluorosulfonic acid ionomer (Nafion). The catalyst layer has a homogeneous thickness of approximately $7 \mu\text{m}$ and a porous structure as shown in Fig. 1B. Fig. 1C further shows that the internal structure of the catalytic layer consisting of Pt/C agglomerates, which is consistent with the previous report [3,14], and the secondary pores [3] are located between these agglomerates. The catalyst layers with rich pores are beneficial to the water and reaction gas transfer.

3.2. Influence of NFP on ECSA of catalyst layers

Fig. 2A shows the cyclic voltammetric curves obtained in single cell tests (Pt loading of 0.35 mg cm^{-2}). The ECSA was calculated through measuring the charge collected in the hydrogen adsorption/desorption region after double-layer correction and assuming a value of $210 \mu\text{C cm}^{-2}$ for the adsorption of a hydrogen monolayer [15,16]. Navessin et al. [17] have reported that the ECSA of the catalyst layer slightly depended on NFP. However, at least two different stages in ECSA changes can be observed with increasing NFP in this work. As seen in Fig. 2B, the ECSA increases firstly and then decreases with increase of NFP. The ECSA reaches a maximum at NFP of 30 wt.% and then drops down at NFP of 40 wt.%. As the NFP is further increased to 50 wt.%, the ECSA does not change much, indicating a tendency of ECSA towards steady state when the NFP is over 40 wt.%. At low NFP, the surface of Pt catalysts does not effectively contact the Nafion. In this case, the triple phase

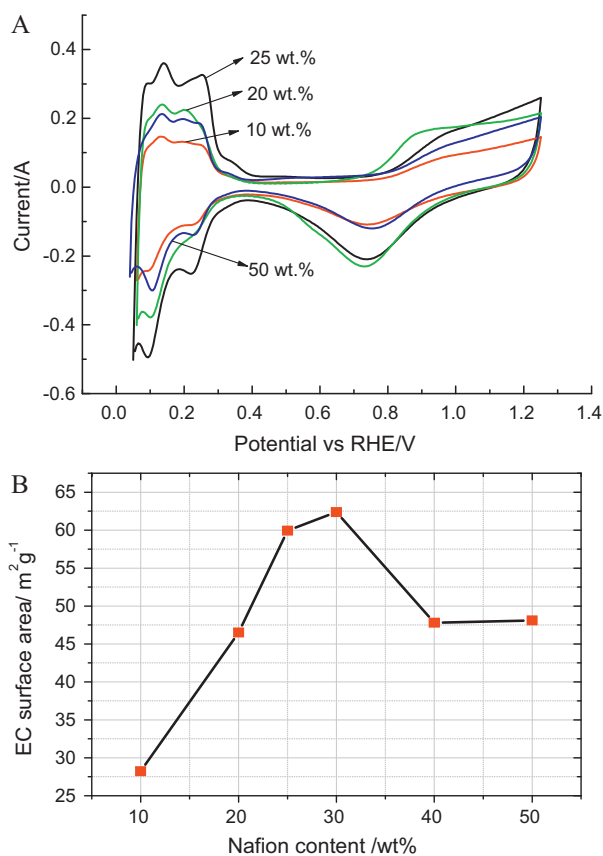


Fig. 2. Cyclic voltammograms (A) and ECSA (B) of Pt catalysts supported on carbon in catalyst layers measured by single cell method with varied NFP at Pt loading of 0.35 and 0.4 mg cm⁻² in cathode and anode, respectively.

boundary reaction zone cannot be formed, which leads to a very low ECSA because of increase of inactive sites [18–20]. With increasing NFP, the ionomer could extend to the surfaces of catalysts and increase the ECSA by forming more triple phase boundary reaction zones. However, the Pt/C agglomerates in catalyst layers could be entirely enveloped by ionomers once the NFP is increased to a threshold value. And then the mass transfer capability of electrodes would be reduced, leading to a decrement of ECSA. If the NFP value is further increased, the ECSA would become constant despite the increase of ionomer thickness. The finding basically confirms the previous results [1,3,4,21], indicating that the negative impact of proton (H⁺) transfer caused by the increased thickness of ionomers is limited.

3.3. Impact of NFP at cathode on fuel cell performance

Single cells with different NFP values in the range of 10–50 wt.% at cathode (Pt loading of 0.35 mg cm⁻²) were assembled. In order to eliminate any possible influences of anode, the NFP value and Pt loading at anode were fixed at 25 wt.% and 0.4 mg cm⁻², respectively. Fig. 3 shows the fuel cell performance at varied NFP values in different polarization regions. In the low current density region of 0–200 mA cm⁻², which is the activation polarization region, the fuel cells with NFP values of 20, 25, 30 and 40 wt.% in catalyst layers exhibit similar performances which are better than those in the case of NFP of 10 and 50 wt.%. The rapid voltage drop in the polarization curve reflects the sluggish kinetics intrinsic to the oxygen reduction reaction at cathode. The triple phase boundary of catalyst layers is reduced under excessively lower NFP (≤ 10 wt.%) condition, whilst the mass transfer resistance increases at higher NFP

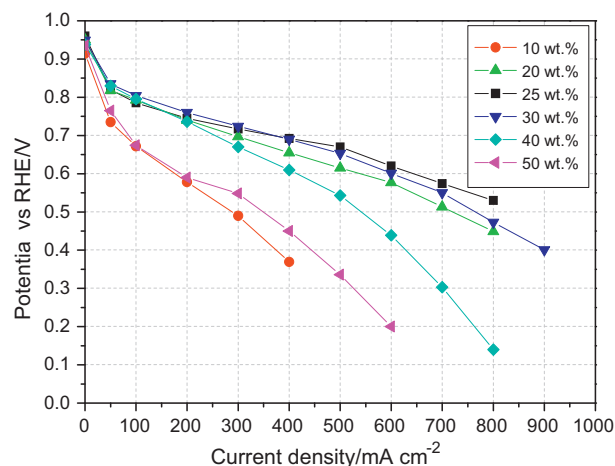


Fig. 3. Effect of NFP at cathode on potential–current.

(≥ 50 wt.%). These could lead to a low catalytic activity of Pt catalysts. In the current density region of 200–700 mA cm⁻², which is an ohmic polarization region of fuel cell operation, the output voltage drops linearly with a small slope in a wide range of output currents. The performance reaches the maximum at NFP value of 25 wt.%, which is slightly higher than that at NFP of 30 and 20 wt.%. A big drop of the performance is observed when the NFP increases to 40 and 50 wt.% or decreases to 10 wt.%. This phenomenon is the most obvious at lower NFP. For the ionomer loadings of 10 wt.% or lower, the absence of enough ionomers as proton transfer pathways in catalyst layers, would cause a larger ohmic resistance. For the higher ionomer loadings, for example the NFP of 40 and 50 wt.%, the specific volume of larger pores in the 0.04–1.0 μ m range are declined [3,22] and water content is increased [17]. It thereby restricts the mass transfer of oxygen and further enlarges the range of concentration polarization region (≥ 300 mA cm⁻²), leading to a considerable reduction of output voltage. On the whole, the fuel cells with NFP of 20–30 wt.% show better performance. However, the cell performance at NFP of 25 and 30 wt.% is almost similar, indicating that the optimum NFP requires the balance between ECSA, ohmic resistance and mass transfer overpotential within the catalyst layer [7,24].

Based on the single cell performance, the samples with NFP values of 20, 25 and 30 wt.% were selected for further study. The oxygen transfer resistance of cathode electrode was characterized by comparing performance of the same fuel cells under either H₂/air and H₂/O₂ conditions [23]. Fig. 4A shows the current–potential polarization curves of cells with NFP of 20, 25 and 30 wt.% under H₂/O₂. The output voltage is 0.60–0.64 V at 800 mA cm⁻². Compared with that under H₂/air condition (0.45–0.53 V at 800 mA cm⁻²), the cell performance is significantly improved under O₂ condition because of the high O₂ concentration at cathode. The cell with NFP of 30 wt.% shows a relatively high performance in comparison with the others. It indicates that the cell with NFP of 30 wt.% in catalyst layer has a strong effect on gas transfer under H₂/O₂ condition. Fig. 4B shows the differential potential curves of cells operated under H₂/air and H₂/O₂. This test is extensively used to evaluate the air transfer resistance in electrodes. Generally, the differential potential is primarily dictated by gas transfer resistance of the catalyst layer with the same gas diffusion layer. Additionally, the cell performance is mainly controlled by the mass transfer at an applied current density of over 800 mA cm⁻². Therefore, the differential potential at 800 mA cm⁻² can be treated as a comparison of air transfer resistance. The results demonstrate that the cell with NFP of 25 wt.% has the least amount

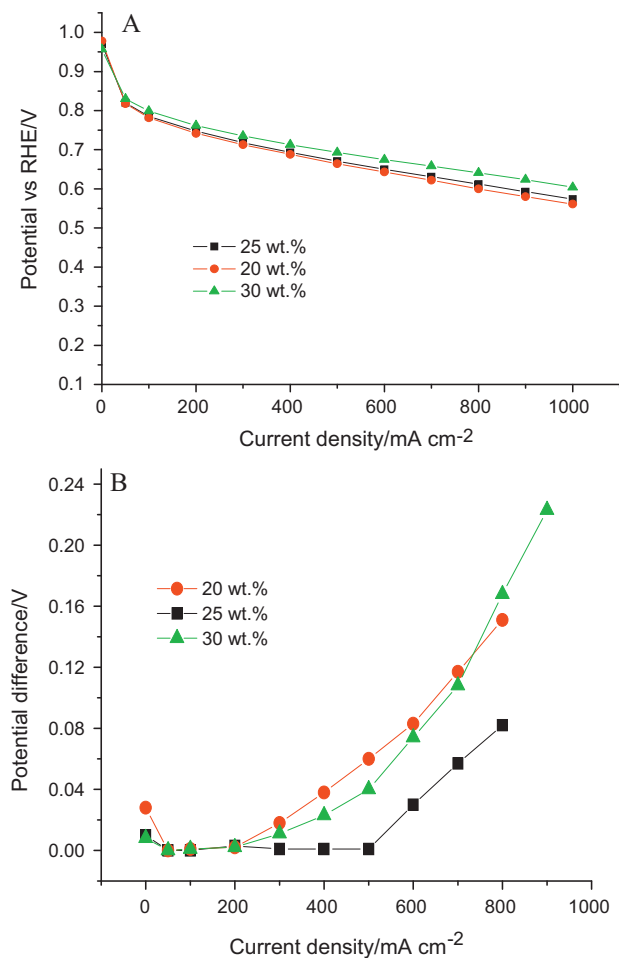


Fig. 4. Effect of NFP at cathode on potential–current (H_2 – O_2) (A) and O_2 transfer resistance (B).

of air transfer resistance as compared to other samples with NFP of 20 and 30 wt.%.

Based on an overall consideration of various factors including ECSA, fuel cell performance and air transfer resistance, the optimum NFP at cathode is in the range of 25–30 wt.%. A high catalytic activity, fuel cell performance and a low air transfer resistance can be obtained in this range.

3.4. Influence of NFP at anode on fuel cell performance

Fig. 5 shows the current–potential curves of single cells with varied NFP at anode and with the NFP of 25% and Pt loading of 0.4 mg cm^{-2} at cathode. It can be seen that the influence of NFP at anode on single cell performance is small in comparison with that at cathode. As the NFP value increases from 10 to 40 wt.%, the cell performance slightly decreases. However, when NFP increases to 50 wt.% the performance decreases significantly. In fact, the anode reaction (hydrogen electro-oxidation) is extremely fast on a catalyst as compared with the cathode reaction (oxygen reduction). Thus, the ECSA of catalyst layers with 10–40 wt.% NFP cannot influence the cell performance. The slow performance degradation with the raised NFP at anode might be caused by a sluggish increase of hydrogen transfer resistance, whilst the rapid performance degradation of the cell with NFP of 50 wt.% could be attributed to the increased impedance of electrodes. Although the cell with NFP of 10 wt.% at Pt loading of 0.35 mg cm^{-2} in anode shows the best performance, the consumption of Pt is very high because of low ECSA of 28.2 g cm^{-2} , as shown in Fig. 2B. By contrast, for the cell with

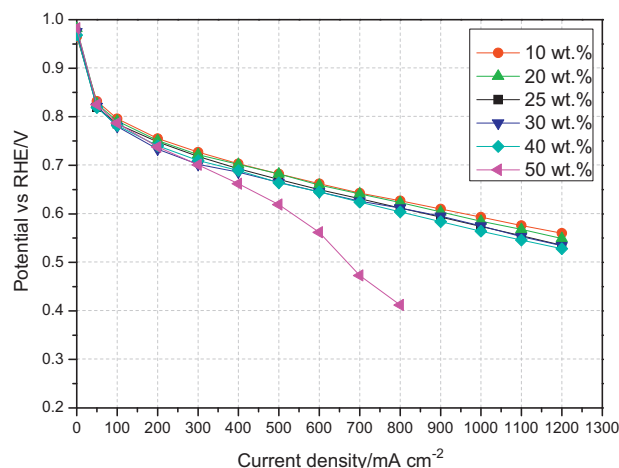


Fig. 5. Influence of anode NFP on potential–current (H_2 – O_2) with the NFP of 25% and Pt loading of 0.4 and 0.35 mg cm^{-2} at cathode and anode, respectively.

NFP of 30 wt.% at the same Pt loading, its ECSA of 62.4 g cm^{-2} is two times as high as that level. It displays that the Pt amount used can be reduced to less than half to obtain the same performance. Thus, it is reasonable to believe that the optimum NFP at anode is 30 wt.%.

3.5. Correlation between Pt loading and NFP at cathode

As discussed above, the reasonable value of NFP at cathode is in the range of 20–30 wt.%. The performance for other samples with NFP of 10 and 50 wt.% is quite low. Therefore, the samples with NFP of 20, 25, 30 and 40 wt.% were used to evaluate the correlation between Pt loading and NFP at cathode. Fig. 6 shows the current–potential polarization curves of cells with the NFP of 20 (Fig. 6A), 25 (Fig. 6B), 30 (Fig. 6C) and 40 wt.% (Fig. 6D) as the Pt loading increases from 0.15 , 0.35 to 0.5 mg cm^{-2} , respectively. As illustrated in Fig. 6A, the output voltage of the cells with NFP of 20 wt.% is improved with increasing Pt loading, and the basically identical situation also appears in the others with NFP of 25–40 wt.% (Fig. 6B–D). However, for the cells with NFP of 25 wt.%, their output voltage is close at Pt loading of 0.35 and 0.5 mg cm^{-2} (Fig. 6B) as the current density is over 400 mA cm^{-2} . Such enhancement of the performance could be attributed to the increased ECSA of catalysts with increasing the amount of Pt.

Fig. 6E shows that the cells with NFP of 25 wt.% always have higher output voltage performance at a given current density of 0.6 A cm^{-2} than that with NFP of 20, 30 and 40 wt.% under increasing Pt loading from 0.15 , 0.35 to 0.50 mg cm^{-2} . This demonstrates that the optimum NFP at cathodes is 25 wt.%, and has no obvious relationship with Pt loading. In addition, it presents a decreased trend of the performance at current density 0.6 A cm^{-2} in the order of the cells with NFP of 25, 30, 20 and 40 wt.% under the same Pt loading. These results are in good agreement on the reports by other researchers, where they have demonstrated the presence of an optimum NFP of 33–40 wt.% (the average optimum NFP value is about 36 wt.%) for 10–25 wt.% Pt/C catalysts (see Table 1). Antolini et al. [7] believed that above NFP of 27 wt.%, by impregnation the Nafion forms a film on external surface of electrode, and it further occupies the space between the catalyst particles up to NFP of 36 wt.%. It is important to note that, in these reports, the Pt loading in catalyst layers was differently distributed from 0.1 to 0.5 mg cm^{-2} , and the existence of an optimum NFP strongly indicates that there is no direct relationship between the Pt loading and optimum NFP. However, this result is opposite to the report by a few researchers such as Sasikumar et al. [5,6] who concluded that

Table 1
Comparison of optimum Nafion loading between literature data.

Reference	Pt (%)	Pt loading (mg cm^{-2})	Optimum NFP (%)
This work	60	0.15, 0.35, 0.50	25–30
Paganin et al. [1]	10	0.4	30–35
Passalacqua et al. [4]	20	0.5	33
Antolini et al. [7]	20	0.2	40
Uchida et al. [3]	25	0.1	33

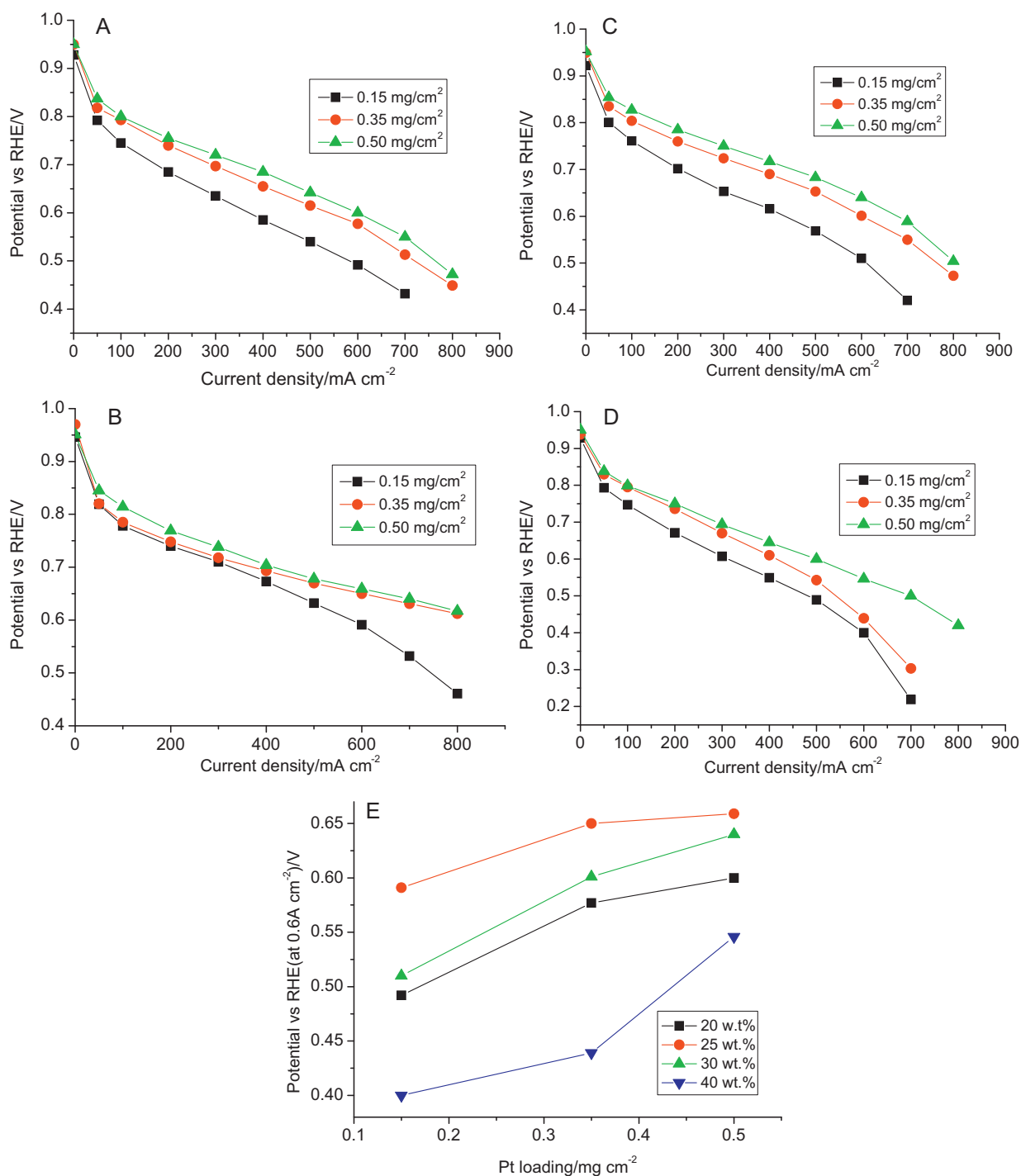


Fig. 6. Cathode potential–current curves with NFP of 20 (A), 25 (B), 30 (C) and 40 wt.% (D) by changing Pt loading from 0.15, 0.35 to 0.5 mg cm^{-2} , and comprehensive performance comparison at 0.6 A cm^{-2} (E).

the optimum NFP in catalyst layers depended on Pt loadings from experimental data. But they did not give a reason explanation.

We have demonstrated that the optimum NFP is irrespective of the Pt loading, and achieved consistency with most of previous research results, however the optimum NFP at cathode is lower than that reported by references. The preliminary view on this change is that the radically increased wt.% of Pt supported on carbon with the same size and dispersion degree of Pt particles (i.e. 60 wt.%) can reduce the usage amount of Nafion due to the decreased distance between Pt particles on supports. Usually, the proton (H^+) formed on Pt surfaces at anode needs to be transferred to catalyst layer–membrane interfaces by recast Nafion films in catalyst layers, whilst it is just the opposite process at cathode electrode. The shortened distance between Pt particles can speed up the H^+ transfer onto Pt surfaces at cathode. In addition, the reduced Nafion usage is benefit for increasing the secondary pores between Pt/C agglomerates [3], leading to improved porosity of catalyst layers and promotion of the oxygen transfer. However, the higher and lower NFP could block the oxygen and hydrogen transfers, respectively. The best performance is obtained for fuel cells with NFP of about 25–30 wt.%, representing an optimum balance of proton transport, oxygen diffusion and ECSA.

4. Conclusions

The percentage of Nafion (NFP), which is one sort of the perfluorosulfonic acid ionomers in catalyst layers of proton exchange membrane fuel cells exhibited an effect on electrochemical surface area (ECSA) of Pt catalysts. The ECSA increased to a maximum and then decreased to a stable value with increase of NFP from 10 to 50 wt.% in fuel cells. The NFP influenced gas transfer resistance significantly. A relatively reasonable gas transfer resistance corresponding to higher performance was obtained for fuel cells with the optimum NFP of 25–30 wt.% at cathode. However, the NFP at anode influenced fuel cell performance slightly. Based on the analysis of the performance and utilization rate of ECSA of Pt catalysts, the optimum NFP in anode was 30 wt.% under low Pt loading condition. In addition, there was no indication showing correlation between the optimum NFP and the Pt loadings at cathode. At all

utilization rates of ECSA, the optimum NFP at cathode was 25–30 wt.%. The results are prospective to improve the fuel cell performance as well as the utilization rate of catalysts.

Acknowledgments

This work was financially supported by the National Natural Science Foundation of China (NSFC) (50972112, and 20876121) and the Major State Basic Research Development Program of China (973 Program) (No. 2012CB215504).

References

- [1] V.A. Paganin, E.A. Ticianelli, E.R. Gonzalez, *J. Appl. Electrochem.* 26 (1996) 297.
- [2] J.M. Song, S.Y. Cha, W.M. Lee, *J. Power Sources* 94 (2001) 78.
- [3] M. Uchida, Y. Aoyama, N. Eda, A. Ohta, *J. Electrochem. Soc.* 142 (1995) 4143.
- [4] E. Passalacqua, F. Lufrano, G. Squadrito, A. Pattia, L. Giorgi, *Electrochim. Acta* 46 (2001) 799.
- [5] G. Sasikumar, J.W. Ihm, H. Ryu, *J. Power Sources* 132 (2004) 11.
- [6] G. Sasikumar, J.W. Ihm, H. Ryu, *Electrochim. Acta* 50 (2004) 601.
- [7] E. Antolini, L. Giorgi, A. Pozio, E. Passalacqua, *J. Power Sources* 77 (1999) 136.
- [8] Z. Qi, A. Kaufman, *J. Power Sources* 113 (2003) 37.
- [9] D. Lee, S. Hwang, *Int. J. Hydrogen Energy* 33 (2008) 2790.
- [10] H.L. Tang, S.L. Wang, M. Pan, R.Z. Yuan, *J. Power Sources* 166 (2007) 41.
- [11] G. Wu, D.Y. Li, C.S. Dai, D.L. Wang, N. Li, *Langmuir* 24 (2008) 3566.
- [12] S. Gottesfeld, M.S. Wilson, *J. Appl. Electrochem.* 22 (1992) 1.
- [13] S.C. Mu, C. Xu, Y. Gao, H.L. Tang, M. Pan, *Int. J. Hydrogen Energy* 35 (2010) 2872.
- [14] X.L. Cheng, B.L. Yi, M. Han, J.X. Zhang, Y.G. Qiao, J.R. Yu, *J. Power Sources* 79 (1999) 75.
- [15] T.J. Schmidt, H.A. Gasteige, G.D. Stäb, P.M. Urban, D.M. Kolb, R.J. Behm, *J. Electrochem. Soc.* 145 (1998) 2354.
- [16] L.C. Ciacchi, W. Pompe, A.D. Vita, *J. Phys. Chem. B* 107 (2003) 1755.
- [17] T. Navessin, M. Eikerling, Q.P. Wang, D.T. Song, Z.S. Liu, J. Horsfall, K.V. Lovell, S. Holdcroft, *Electrochem. Soc.* 152 (2005) A796.
- [18] S. Gottesfeld, I.D. Raistrick, S. Srinivasan, *J. Electrochem. Soc.* 134 (1987) 1455.
- [19] G. Tamizhmani, I.P. Dodelet, D. Guay, *J. Electrochem. Soc.* 143 (1996) 18.
- [20] D.R. Lawson, L.D. Whiteley, C.R. Martin, M.N. Szentirmay, J.I. Song, *J. Electrochem. Soc.* 135 (1988) 2247.
- [21] P. Gode, F. Jaouen, G. Lindbergh, A. Lundblad, G. Sundholm, *Electrochim. Acta* 48 (2003) 4175.
- [22] M. Uchida, Y. Fukuoka, Y. Sugawara, N. Eda, A. Ohta, *J. Electrochem. Soc.* 143 (1996) 2245.
- [23] T.H. Yang, Y.G. Yoon, G.G. Park, W.Y. Lee, C.S. Kim, *J. Power Sources* 127 (2004) 230.
- [24] D.T. Song, Q.P. Wang, Z.S. Liu, M. Eikerling, Z. Xie, T. Navessin, S. Holdcroft, *Electrochim. Acta* 50 (2005) 3347.